10th AIAA/CEAS Aeroacoustics Conference, 10-12 May 2004, Manchester, UK

Modeling of Synthetic Anisotropic Turbulence and Its Sound Emission

Mattias Billson *and Lars-Erik Eriksson †and Lars Davidson†
Chalmers University of Technology, SE-412 96 Göteborg, Sweden
and Peter Jordan ‡
LEA UMR-CNRS 6609, Poitiers, France

Synthetic turbulence is an important component in several applications. In advanced hybrid LES-RANS approaches it can be used as an interface forcing condition between the RANS and the LES and in LES it can be used to set up time dependent inflow boundary conditions. In these methods the anisotropy of the synthesized turbulence is important in order to get the proper excitation of the unsteady computations. Within the context of the present work realizations of synthesized turbulence are used as source fields for a hybrid approach for jet noise predictions. In this application the anisotropy is an important factor for the noise generation. A method is presented in which anisotropic synthesized turbulence can be generated from isotropic synthesized turbulence. The method is based on scaling and transformation of isotropic turbulence so that the anisotropy is the same as that of an arbitrary specified Reynolds stress tensor. In the present approach the resulting velocity fields will be anisotropic in velocities as well as in length scales. The resulting velocity field is divergence free for homogeneous flows. In this work the method is used to generate anisotropic turbulence in a box and the near-field statistics are evaluated. The method is found to be able to simulate the anisotropy of a specified Reynolds stress tensor. The length scale anisotropy in the synthesized turbulence is found to be aligned with the directions of the normal Reynolds stress tensor components. The noise emission from the generated turbulence is computed through the inhomogeneous linearized Euler equations (ILEE) together with a Kirchhoff surface to extend the solution to the far-field. Also, a statistical model based on Lighthill's acoustic analogy is used to compute the noise emitted by the anisotropic turbulence and the predicted sound from the synthesized turbulence is compared with the statistical model.

Nomenclature

Roman letters

$\mathbf{a}$	normalized Reynolds stress tensor
c	speed of sound
f	frequency
f_A	amplitude factor
$\mathbf{r}$	spatial separation vector, $\mathbf{x} - \mathbf{x}'$

*PhD student, Division of Thermo and Fluid Dynamics, Department of Mechanical Engineering
†Professor, Division of Thermo and Fluid Dynamics, Department of Mechanical Engineering
‡Chargé de Recherche (Researcher), Laboratoire d'Etudes Aérodynamiques UMR-CNRS 6609

$f(r)$	longitudinal correlation function
I	unitary tensor
k	wave number length
$\mathbf{k}$	wave number vector
$\overline{k}$	turbulence kinetic energy
L	length scale
L_t	turbulence length scale
p	pressure
r	length of $\mathbf{r}$
$\mathbf{R}$	rotation matrix
$\mathbf{R}_{ij}$	$\mathbf{R}_{ij}(\mathbf{y}, \mathbf{r})$ second order correlation tensor (zero time separation)
$\mathbf{R}_{ijkl}$	$\mathbf{R}_{ijkl}(\mathbf{y}, \mathbf{r}, \tau)$ fourth order correlation tensor
$\mathbf{R}_{ij}$	$\mathbf{R}_{ij}(\mathbf{y}, \mathbf{r}, \tau)$ second order correlation tensor
$\mathbf{T}$	Reynolds stress tensor
$\mathbf{u}$	velocity fluctuation
$\hat{u}$	mode amplitude
$\mathbf{v}$	velocity fluctuation
$\mathbf{x}$	spatial coordinate
x_i	observer location
$\mathbf{xyz}$	coordinate system
$\mathbf{y}$	spatial coordinate

Greek letters

Δt	time step
ω_b	angular frequency scale
ψ	phase angle
ρ	density
$\boldsymbol{\sigma}$	direction vector
τ	time separation
$\boldsymbol{\tau}$	Reynolds stress tensor
τ_t	turbulence time scale
θ	angle from x-axis in xy-plane

Subscripts

0	ambient
amb	ambient conditions
n	mode number
rms	root-mean-square

Superscripts

a	anisotropic
$*$	expressed in principal axes of $\boldsymbol{\tau}$
i	isotropic
m	time step number
$\underline{T}$	transpose
$\overline{(\cdot)}$	average

I. Introduction

Synthesized turbulence is in the present work used to generate source fields for the inhomogeneous linearized Euler equations with the purpose of performing noise predictions of turbulent velocity fields.

Until now only isotropic synthesized turbulence has been considered for this purpose.[1–4]

A method to model anisotropic synthetic turbulence has been developed in the present work and this paper is focused on evaluating the properties of the newly developed method. The same method to introduce anisotropy in synthesized turbulence was previously presented by Smirnov *et al.*[5] The procedure to generate anisotropic turbulence in [5] is called RFG (Random Flow Generation) and has several elements in common with the method presented in this paper. A modified version of the one presented in [5] has recently been presented by Batten *et al.*[6] A full presentation of the method to introduce anisotropy in the framework of the present work will be given.

In [5] the randomly generated anisotropic turbulence was used for initial and inlet boundary conditions for LES (Large Eddy Simulation) and for particle tracking in LES/RANS (Reynolds Averaged Navier-Stokes) computations. Of special interest in the present work is the spatial structure as well as the sound generation properties of the synthesized anisotropic turbulence. Both near-field turbulence statistics and far-field acoustic statistics of the synthesized turbulence are evaluated.

The structure of the paper is as follows. The theory of transforming an isotropic Reynolds stress tensor into an anisotropic one is first presented. This is followed by a description of how to generate anisotropic synthesized velocity fields. Different aspects of anisotropy in terms of velocities, length and time scales are then discussed. This is followed by a numerical experiment from which near and far-field results are evaluated. The far-field results are also compared to a Lighthill's analogy[7] based statistical model. The numerical results are computed through the inhomogeneous linearized Euler equations[8] together with a Kirchhoff surface[9] and the statistical results are based on a modified version of Ribner's model for isotropic turbulence.[10] This is followed by conclusions from the results.

II. Synthesis of Anisotropic Turbulence

In this section it will be shown how it is possible to synthesize a turbulent velocity field which has any specified anisotropy in terms of Reynolds stresses using stochastically generated isotropic turbulence. First the analysis will be made on stress tensors, i.e. the time averaged Reynolds stress tensor. Then the method of producing velocity fields with the appropriate properties will be shown.

A. Stress Tensor Analysis

For any turbulent velocity field $\mathbf{u}$ which is anisotropic and given a coordinate system $\mathbf{xyz}$ there is a Reynolds stress tensor

$$\boldsymbol{\tau} = -\overline{\rho \mathbf{u}\mathbf{u}^T} \tag{1}$$

where overline denotes average and the off-diagonal elements are not necessarily equal to zero. Since the Reynolds stress tensor is symmetric, there is a coordinate system $\mathbf{xyz}^*$ in which the off-diagonal elements in the tensor are equal to zero. This is called the principal coordinate system related to the stress tensor and is denoted by the superscript $(\cdot)^*$. This tensor can be constructed as

$$\boldsymbol{\tau}^* = \mathbf{R}^T \boldsymbol{\tau} \mathbf{R} \tag{2}$$

where $\mathbf{R}$ is a matrix containing the three eigenvectors of $\boldsymbol{\tau}$ in the columns and $\mathbf{R}^T$ is the transpose of $\mathbf{R}$. The tensor $\boldsymbol{\tau}^*$ contains the eigenvalues of $\boldsymbol{\tau}$ in the diagonal. The $\mathbf{R}$ matrix is a rotation matrix which rotates the velocity field from $\mathbf{xyz}$ to $\mathbf{xyz}^*$. Since the trace of $\boldsymbol{\tau}$ is equal to $-2\overline{\rho k}$ where $\overline{\rho k}$ is the average turbulence kinetic energy we can define an normalized stress tensor

$$\mathbf{a} = -\frac{3}{2}\frac{\boldsymbol{\tau}}{\overline{\rho k}} \tag{3}$$

which in the principal coordinate system is given by

$$\mathbf{a}^* = \mathbf{R}^T \mathbf{a} \mathbf{R} \tag{4}$$

The degree of anisotropy in $\boldsymbol{\tau}$ (and $\mathbf{a}$) is the same in any coordinate system and is unambiguously defined by the diagonal components in $\mathbf{a}^*$.

The stress tensor $\mathbf{T}^i$ associated with an isotropic velocity field $\mathbf{u}^i$ is given by

$$\mathbf{T}^i = -\overline{\mathbf{u}^i \mathbf{u}^{iT}} = -\frac{2}{3}\overline{\rho k}\mathbf{I} \tag{5}$$

where $\mathbf{I}$ is the unitary matrix, and superscript $(\cdot)^i$ denotes isotropic. Rotating the tensor $\mathbf{T}^i$ to the principal axes of $\boldsymbol{\tau}$ gives

$$\mathbf{T}^{i*} = \mathbf{R}^T \mathbf{T}^i \mathbf{R} = -\mathbf{R}^T \frac{2}{3}\overline{\rho k}\mathbf{I}\mathbf{R} = \mathbf{T}^i \tag{6}$$

The stress tensor $\mathbf{T}^i$ is clearly unchanged by rotation since it is a scaled unitary matrix but the rotated tensor $\mathbf{T}^{i*}$ is formally oriented in the principal axes of $\boldsymbol{\tau}$.

The goal is to make the isotropic tensor $\mathbf{T}^i$ anisotropic, i.e. to create an anisotropic tensor $\mathbf{T}^a$ which is expressed in the original coordinate system, where the superscript $(\cdot)^a$ denotes anisotropic. This is done in two steps. First by scaling $\mathbf{T}^{i*}$ with the normalized stress tensor $\mathbf{a}^*$ as

$$\mathbf{T}^{a*} = \mathbf{a}^* \mathbf{T}^{i*} \tag{7}$$

The stress tensor $\mathbf{T}^{a*}$ will thus inherit the anisotropy of $\boldsymbol{\tau}^*$. This can be seen by

$$\begin{aligned} \mathbf{T}^{a*} = \mathbf{a}^* \mathbf{T}^{i*} &= \mathbf{a}^* \left(-\frac{2}{3}\overline{\rho k}\mathbf{I} \right) \\ &= \left(-\frac{3}{2}\frac{\boldsymbol{\tau}^*}{\overline{\rho k}} \right) \left(-\frac{2}{3}\overline{\rho k}\mathbf{I} \right) = \boldsymbol{\tau}^* \end{aligned} \tag{8}$$

Secondly by transforming $\mathbf{T}^{a*}$ back to the original coordinate system **xyz** using

$$\mathbf{T}^a = \mathbf{R}\mathbf{T}^{a*}\mathbf{R}^T = \mathbf{R}\boldsymbol{\tau}^*\mathbf{R}^T = \boldsymbol{\tau} \tag{9}$$

the stress tensor $\mathbf{T}^a$ will be an anisotropic tensor with the same anisotropy as the Reynolds stress tensor $\boldsymbol{\tau}$. In Eqs. (1) to (9) it is shown that an isotropic stress tensor $\mathbf{T}^i$ associated with the velocity field $\mathbf{u}^i$ can be transformed to an anisotropic stress tensor $\mathbf{T}^a$ with the same anisotropy as the known model anisotropic stress tensor $\boldsymbol{\tau}$.

B. How-to and Considerations

In this subsection it will be shown how velocity fields with a specified anisotropic Reynolds stress tensor are generated based on stochastically generated isotropic velocity fields. A statistically isotropic velocity field can be generated using[1, 11, 12]

$$\mathbf{u}^i(\mathbf{x}) = 2\sum_{n=1}^{N} \hat{u}_n \cos(\mathbf{k}_n \cdot \mathbf{x} + \psi_n)\boldsymbol{\sigma}_n \tag{10}$$

where $\hat{u}_n$, $\mathbf{k}_n$, ψ_n, $\boldsymbol{\sigma}_n$ are the amplitude, wave number, phase and direction in physical space of mode number n. The amplitude $\hat{u}_n$ of each mode is computed from a model of the isotropic energy spectrum function, e.g. a von Kármán-Pao spectrum.[1, 13] The wave number, phase and direction in physical space involve random functions to ensure isotropy. The velocity field generated by Eq. (10) will have an isotropic stress tensor

as in Eq. (5) and it will be free of divergence if $\mathbf{k}_n$ and $\boldsymbol{\sigma}_n$ are orthogonal, i.e. $\mathbf{k}_n \cdot \boldsymbol{\sigma}_n = 0$. For more details on the generation of isotropic synthetic turbulence, see Billson *et al.*[1,12] The same velocity field can be expressed in the principal coordinate system $\mathbf{xyz}^*$ of the model stress tensor $\boldsymbol{\tau}$ as

$$\mathbf{u}^{i*}(\mathbf{x}^*) = \mathbf{R}^T \mathbf{u}^i(\mathbf{x}) = 2 \sum_{n=1}^{N} \hat{u}_n \cos(\mathbf{k}_n^* \cdot \mathbf{x}^* + \psi_n) \boldsymbol{\sigma}_n^* \tag{11}$$

where

$$\boldsymbol{\sigma}_n^* = \mathbf{R}^T \boldsymbol{\sigma}_n \quad ; \quad \mathbf{k}_n^* = \mathbf{R}^T \mathbf{k}_n \tag{12}$$

The stress tensor of $\mathbf{u}^{i*}(\mathbf{x}^*)$ will be as in Eq. (6), i.e. the same as in 5 but now in the coordinate system $\mathbf{xyz}^*$.

A velocity field $\mathbf{u}^{a*}(\mathbf{x}^*)$ which is anisotropic is constructed by scaling the velocity field $\mathbf{u}^{i*}(\mathbf{x}^*)$ by $\mathbf{a}^{*1/2}$ as

$$\mathbf{u}^{a*}(\mathbf{x}^*) = \mathbf{a}^{*1/2} \mathbf{u}^{i*}(\mathbf{x}^*) = 2 \sum_{n=1}^{N} \hat{u}_n \cos(\mathbf{k}_n^{a*} \cdot \mathbf{x}^* + \psi_n) \boldsymbol{\sigma}_n^{a*} \tag{13}$$

where

$$\boldsymbol{\sigma}_n^{a*} = \mathbf{a}^{*1/2} \boldsymbol{\sigma}_n^* \tag{14}$$

is the scaled direction of the n:th mode, and $\mathbf{a}^*$ is the normalized stress tensor in the principal coordinate system associated with the model Reynolds stress tensor $\boldsymbol{\tau}$. The square root denotes the square root of each element. The wave number $\mathbf{k}_n^{a*}$ in Eq. (13) is defined by

$$\mathbf{k}_n^{a*} = \mathbf{a}^{*-1/2} \mathbf{k}_n^* \tag{15}$$

This modified wave number is introduced to make sure that the resulting velocity field will have zero divergence, i.e. $\mathbf{k}_n^{a*} \cdot \boldsymbol{\sigma}_n^{a*} = 0$. The stress tensor associated with $\mathbf{u}^{a*}(\mathbf{x}^*)$ is given by

$$\mathbf{T}^{a*} = -\mathbf{u}^{a*} \mathbf{u}^{a*T} = -\mathbf{a}^{*1/2} \mathbf{u}^{i*} \mathbf{u}^{i*T} \mathbf{a}^{*1/2^T} = \mathbf{a}^{*1/2} \mathbf{T}^{i*} \mathbf{a}^{*1/2^T} \tag{16}$$

and since $\mathbf{T}^{i*}$ is a unitary tensor one can write

$$\mathbf{T}^{a*} = \mathbf{a}^* \mathbf{T}^{i*} \tag{17}$$

which is the same relation as in Eq. (7) and relation 8 follows. Thus the stress tensor associated with the velocity field $\mathbf{u}^{a*}(\mathbf{x}^*)$ has the same anisotropy as the model tensor $\boldsymbol{\tau}^*$. The final expression for the anisotropic velocity field expressed in the original coordinate system $\mathbf{xyz}$ is simply computed by

$$\mathbf{u}^a(\mathbf{x}) = \mathbf{R} \mathbf{u}^{a*}(\mathbf{x}^*) \tag{18}$$

III. Time Evolution

To evolve the turbulence in time a filter operator is used.[1,12] This filter operator uses statistically independent velocity fields $\mathbf{u}^m(\mathbf{x})$ generated by Eq. (13) (and Eq. (18)) as input and ensures a specified autocorrelation of the output signal $\mathbf{v}^m(\mathbf{x})$. The filter is given by

$$\mathbf{v}^m(\mathbf{x}) = a \mathbf{v}^{m-1}(\mathbf{x}) + b(\mathbf{u}^m(\mathbf{x}) + \mathbf{u}^{m-1}(\mathbf{x})) \tag{19}$$

where $a = \exp(-\Delta t/\tau_t)$, $b = f_A \sqrt{(1-a)/2}$ and Δt and τ_t are the time step size and the time scale respectively. Superscript $(\cdot)^m$ denotes time step number and f_A is an amplitude factor to enable control of the kinetic energy of the synthesized turbulence.

IV. Classification of Anisotropy

The anisotropy of the Reynolds stress tensor can be expressed using the Lumley triangle[14] based on the invariants of $\boldsymbol{\tau}$. This notation of the anisotropy is however not chosen here. Instead, the anisotropy is chosen to be expressed in terms of the normalized tensor $\mathbf{a}^*$ in the principal axes. The reason for this is that the sound generation directivity from homogeneous turbulence without convection is aligned with the principal axes of the stress tensor as will be shown by the results below.

For homogeneous turbulence, three forms of anisotropy can be identified. These are velocity fluctuation, length and time scale anisotropy. The velocity anisotropy can easily be identified in the Reynolds stress tensor which is a one-point statistical property of the flow. The length and time scale anisotropy respectively are however correlation properties which require two-point statistics in space and/or time. The proposed method to generate synthesized turbulence includes anisotropy in velocity and length scale but not time scale. The properties of this synthesized anisotropic turbulence will be presented below through a numerical test case.

V. Numerical Experiment

The numerical experiment consists of a box with a width of one meter with 128 equally sized cells in each direction. The center 64 cube cells define the source region, see Fig. 1. In this region, synthesized turbulence is generated and used to evaluate source terms for the inhomogeneous linearized Euler equations on conservative form[8] which are solved for in the entire box. The reference solution in the box is that of stagnant air with ambient density of $\rho_0 = 1.2$ kg/m^3 and pressure $p_0 = 100\,000$ Pa, i.e. there is no shear in the mean solution. Only the specified Reynolds stress tensors used in the synthesis of the source fields include effects of anisotropy in the experiment. Two different anisotropic turbulence fields will be presented. One (case 1) with the anisotropy in the **xy**-plane and the principal axes aligned with the **xyz** coordinate system. The other (case 2) has the same degree of anisotropy but the principal axes are rotated by 45 degrees in the **xy**-plane.

The input turbulence kinetic energy and dissipation rate for the synthesized turbulence are $\overline{k} = 763$ m^2/s^2 and $\varepsilon = 763 \times 10^3$ m^2/s^3 respectively. The length scale, time scale and amplitude factors are set to $f_L = 1$, $f_\tau = 3$ and $f_A = 1$. This gives a turbulence with time and length scales[1] of the synthesized turbulence equal to $(\tau_t, L_t) = (0.003, 0.028)$ [s, m].

The acoustic solution which propagates out from the source region is integrated close to the outer boundary using the Kirchhoff[9] method to extend the solution to observer positions at a distance of 100 meters from the box. These observers are positioned on circles with 36 locations oriented in the coordinate system axis planes. The numerical schemes in the numerical experiment are described in Billson *et al.*[1,13]

For two-point statistics special grids were used which consisted of tubes with $128 \times 1 \times 1$ cells oriented in different directions in which large numbers of samples could be generated. The mesh spacing in these tubes were the same as in the box test case.

VI. Near-Field Evaluation

A. Velocity anisotropy

The anisotropy of the velocity components for case 1 is in terms of normalized Reynolds stresses shown in table 1. To the left is the normalized Reynolds stress tensor which is the model stress tensor in case 1, and to the right is the stress tensor which is sampled from 100 000 samples from the SNGR method. In table 2 the model tensor in case 2 is shown, and the resulting stress tensor from the SNGR is to the right. The proposed method to generate anisotropic turbulence can clearly model an anisotropic Reynolds stress tensor, both when specified in the principal axes (case 1) and when rotated (case 2). Observe that the degree of anisotropy is the same in the two cases.

An illustrative plot of anisotropy is shown in Fig. 2 displaying scatter plots from DNS and synthesized

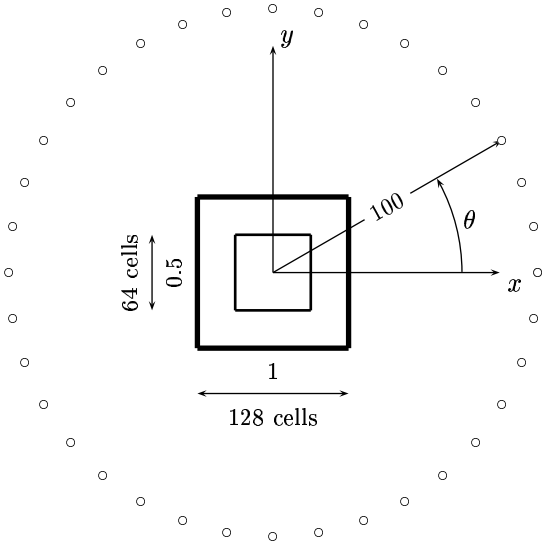

Figure 1. xy-plane of computational domain with 36 observer points. Small box: SNGR source region; Large box: LEE domain

Table 1. Normalized Reynolds stress tensor elements. Case 1 Left: model tensor; Right: sampled from SNGR method.

1.5	0	0	1.499	0.002	−0.003
0	0.5	0	0.002	0.495	0.002
0	0	1	−0.003	0.002	1.005

Table 2. Normalized Reynolds stress tensor elements. Case 2 Left: model tensor; Right: sampled from SNGR method.

1	0.5	0	0.998	0.494	−0.005
0.5	1	0	0.494	0.996	0.003
0	0	1	−0.005	0.003	1.006

turbulence with the same degree of anisotropy. The DNS data in Fig. 2(a) are taken from fully developed channel flow at $y^+ = 60$ and has a normalized Reynolds stress tensor as in table 3. As expected, there is a preferred occurrence of scatter dots in quadrants 2 and 4 (with opposite signs of u and v) reflecting the negative cross correlation $\mathbf{a}_{12} = -0.37$ in table 3. This is also the case for the synthesized anisotropic turbulence in Fig. 2(b).

Table 3. Normalized Reynolds stress tensor for channel flow DNS at $y^+ = 60$

1.91	−0.37	0
−0.37	0.39	0
0	0	0.70

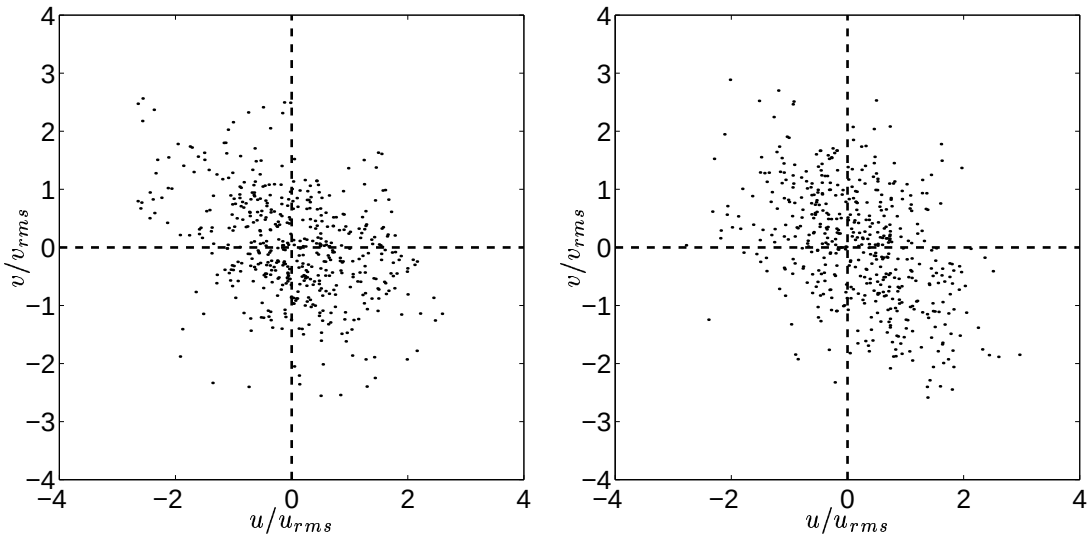

(a) DNS data

(b) Synthesized anisotropic turbulence

Figure 2. Scatter plot of u and v fluctuations.

A realization of the synthetic anisotropic velocity field for case 2 is shown in Fig. 3(a). The vectors are the velocity components and the gray-scale is the w-component out of the paper. The preferred direction with large vector components are oriented in the 45 degree angle relative to the positive x-axis. This reflects the normalized stress tensor component $\mathbf{a}_{12} = 0.5$. The opposite is true with small vector components in the -45 degree angle. Figure 3(b) shows the contours of the pressure disturbances which are propagating out from the source region toward the boundary of the box. The directivity of the generated sound can be seen as the longer wave lengths in the 45 degree direction compared to the -45 degree direction.

B. Length scale anisotropy

The longitudinal two-point correlation function (u velocity) with separation i x-direction for case 1 is shown in Fig. 4(a). The transversal two-point correlation function (v velocity) for the same case is also plotted in Fig. 4(a). Also shown as reference are the corresponding correlations for the isotropic case. As can be seen, the length scale in the x-direction increases for both the longitudinal and transversal correlations as the diagonal Reynolds stress tensor component $\overline{\rho uu}$ increases. The u and v velocity two-point correlation in the y-direction for the case 1 are shown in Fig. 4(b) as well as the corresponding correlations for the isotropic case. The correlations in the y-direction are clearly lowered by the anisotropy corresponding to a decrease in the Reynolds stress tensor component $\overline{\rho vv}$.

The longitudinal and transversal two-point correlations for the same case (case 1) as above but in the axes where the normal components of the Reynolds stress tensor are equal (45 degrees) are shown in Fig. 5 as well as the correlations for the isotropic case. The longitudinal and transversal correlations are in this direction close to those of the isotropic case. The change in the length scales in the anisotropic synthesized turbulence is a result of the modified wave number in Eq. (15). The important thing to notice is that the model increases all correlations in the direction of the increased normal component of the normalized stress tensor and vice versa. Also, in a direction with equal normal components of the stress tensor (Fig. 5) the length scales are less changed by the anisotropy of the turbulence. A conclusion which can be drawn from the model is that the orientation of the anisotropy of the length scales can be deduced from the relative

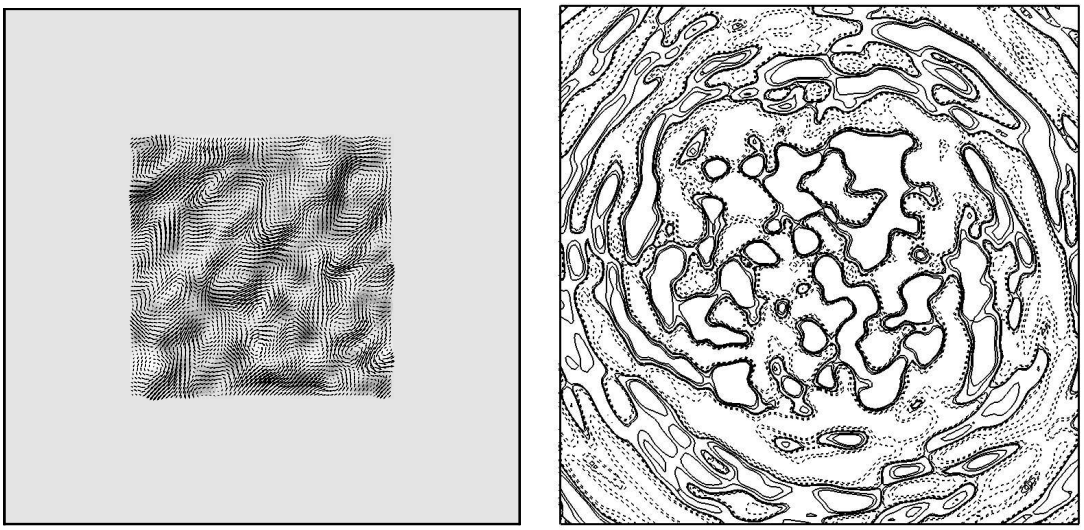

(a) Synthetic anisotropic turbulence. Case 2. Vectors: velocities; gray-scale: w velocity out from paper.

(b) Pressure from ILEE solution. Solid lines: positive values; dashed lines: negative values.

Figure 3. Slice in xy-plane through computational domain

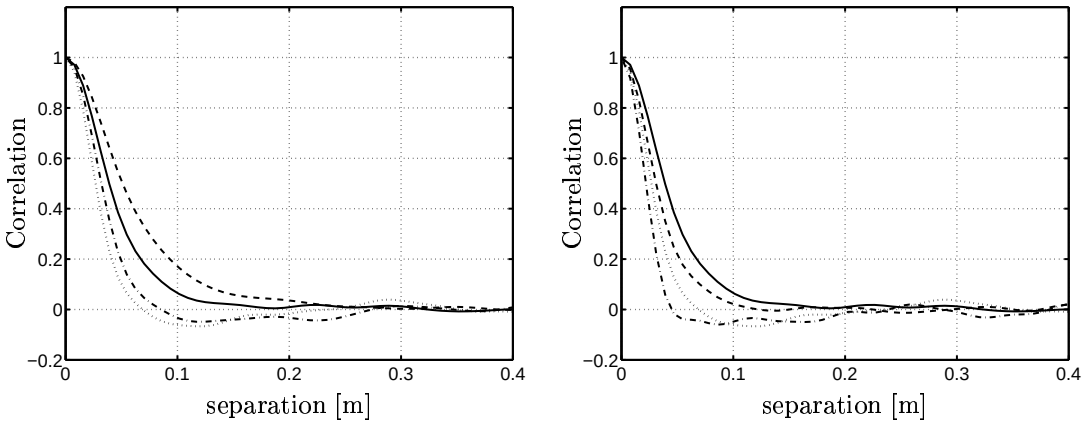

(a) Two-point correlations in x^*-direction

(b) Two-point correlations in y^*-direction

Figure 4. Two-point correlations along principal axes. Dashed line: longitudinal anisotropic ; solid line: longitudinal isotropic; dash-dotted line: transversal anisotropic; dotted line: transversal isotropic

magnitudes of the normal components of the Reynolds stress tensor. The maximum and minimum length scales are thus found in the directions of the principal axes of the Reynolds stress tensor.

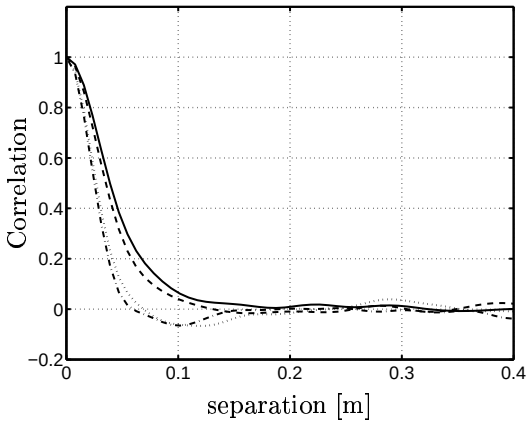

Figure 5. Two-point correlations in 45 degree direction from x^*. Dashed line: longitudinal anisotropic ; solid line: longitudinal isotropic; dash-dotted line: transversal anisotropic; dotted line: transversal isotropic

C. Time scale anisotropy

The present method does not have a time scale anisotropy. This is a possible deficiency for the present method. It is though unclear if there is any strong time scale anisotropy in shear flows. Results from processing of data from LES computations of a high Mach number jet (Andersson *et al.*[15]) indicate that there is a time scale anisotropy in the shear layer of a developing jet but that it is weak compared to the anisotropy in length scale and velocity, see Billson *et al.*[12]

VII. Statistical model – Lighthill's Analogy

Evaluation of the far-field generated noise from the anisotropic synthesized turbulence is done using a statistical Lighthill's analogy based method.[7,10] The model of the sound field intensity generated by localized homogeneous turbulence with zero mean flow can be written as (Ribner[10])

$$I(\mathbf{x}) = \int_{\infty} I(\mathbf{x},\mathbf{y})\mathrm{d}^3\mathbf{y} \tag{20}$$

where

$$\begin{aligned} I(\mathbf{x},\mathbf{y}) &= A\frac{x_i x_j x_k x_l}{x^4}\int_{\infty}\frac{\partial^4}{\partial\tau^4}\mathbf{R}_{ijkl}(\mathbf{y},\mathbf{r},\tau)\mathrm{d}^3\mathbf{r} \\ \mathbf{R}_{ijkl}(\mathbf{y},\mathbf{r},\tau) &= \overline{v_i v_j v_k' v_l'} \\ v_i &= v_i(\mathbf{y},t) \qquad v_k' = v_k(\mathbf{y}+\mathbf{r},t+\tau) \end{aligned} \tag{21}$$

where $A = \rho_0/(16\pi^2 c_0^5 x^2)$. Assuming that velocities at different locations have a joint normal probability distribution, the spatial fourth order correlation $\mathbf{R}_{ijkl}(\mathbf{y},\mathbf{r},\tau)$ can be expressed in terms of two-point second order correlations[16] as

$$\mathbf{R}_{ijkl}(\mathbf{y},\mathbf{r},\tau) = \overline{v_i v_j}\,\overline{v_k v_l} + \mathbf{R}_{ik}\mathbf{R}_{jl} + \mathbf{R}_{il}\mathbf{R}_{jk} \tag{22}$$

where $\mathbf{R}_{ik} = \mathbf{R}_{ik}(\mathbf{y},\mathbf{r},\tau)$. The first term $\overline{v_i v_j}\,\overline{v_k v_l}$ in Eq. (22) is independent of the time separation τ and can be omitted in the analysis. A factorization of $\mathbf{R}_{ij}(\mathbf{y},\mathbf{r},\tau)$ into a space factor and a time factor was postulated by Ribner as

$$\mathbf{R}_{ij}(\mathbf{y},\mathbf{r},\tau) = \mathbf{R}_{ij}(\mathbf{y},\mathbf{r})g(\tau) \tag{23}$$

where $\mathbf{R}_{ij}(\mathbf{y},\mathbf{r}) = \mathbf{R}_{ij}(\mathbf{y},\mathbf{r},\tau = 0)$ is the two-point velocity correlation tensor with zero time separation between the points $(\cdot)$ and $(\cdot)'$ and $g(\tau)$ is the time factor.

An expression for the isotropic velocity correlation tensor derived by Batchelor[16] reads

$$\mathbf{R}_{ij}(\mathbf{r}) = \mathbf{R}_{ij}(\mathbf{y},\mathbf{r}) = u^2 \left[\left(f(r) + \frac{r}{2}\frac{df(r)}{dr} \right) \delta_{ij} - \frac{1}{2}\frac{df(r)}{dr}\frac{r_i r_j}{r} \right] \tag{24}$$

where u^2 is the magnitude of the isotropic normal Reynolds stress and r is the length of the separation vector $\mathbf{r}$. There is no summation over indices in Eq. (24). As a way to introduce anisotropy in the model for the correlation tensor, a modified version of the isotropic velocity correlation tensor is written as

$$\mathbf{R}_{ij}(\mathbf{r}) = \mathbf{R}_{ij}(\mathbf{y},\mathbf{r}) = \overline{u_i u_j} \left[\left(f(r) + \frac{r}{2}\frac{df(r)}{dr} \right) \delta_{ij} - \frac{1}{2}\frac{df(r)}{dr}\frac{r_i r_j}{r} \right] \tag{25}$$

Equation (25) is not formally a proper tensor and does not allow rotation of the coordinate system, but it is still used as an approximate estimation of the sound directivity from anisotropic turbulence when expressed in the principal axes. The longitudinal correlation function $f(r)$ is given the form

$$f(r) = e^{-r^2/L^2} \tag{26}$$

following Lilley.[17] The length scale anisotropy in Eq. (26) is modeled as (Jordan and Gervais[18])

$$L(L_1, L_2, L_3, \mathbf{r}/r) = \sqrt{\frac{L_1^2 L_2^2 L_3^2 (r_1^2 + r_2^2 + r_3^2)}{L_2^2 L_3^2 r_1^2 + L_1^2 L_3^2 r_2^2 + L_1^2 L_2^2 r_3^2}} \tag{27}$$

where the length scales $L_1 = 0.064$ m, $L_2 = 0.040$ m and $L_3 = 0.050$ m are the integral length scales associated with the longitudinal two-point correlations in the x, y and z directions respectively.

The fourth derivative of the temporal correlation is simply modeled as [10]

$$\frac{\partial^4}{\partial \tau^4} g(\tau) = C_t \omega_b^4 \tag{28}$$

where ω_b is a typical angular frequency scale, here computed as $2\pi/\tau_t$ where τ_t is the time scale of the synthesized turbulence. The constant C_t is used to adjust the level of the sound emission.

By introducing spherical coordinates for the observer locations x_i and evaluating Eq. (21) over a correlation volume, the sound directivity from a unit volume can be computed. Equation (20) is then computed as the result from Eq. (21) scaled by the volume of the source region in the numerical experiment. Only the self-noise components[10] of the generated sound from the theory are retained in the following numerical examples. The reason for this is discussed at the end of the results.

VIII. Far-field Evaluation

The OASPL (Over-All Sound Pressure Level) of the emitted sound from the anisotropic turbulence in case 1 is shown in Fig. 6(a) at 36 observer locations on a circle in the **xy**-plane at a radius of 100 m. The sound directivity shows that there is a direction of maximum sound emission in the x-direction and a minimum in the y-direction. This reflects the difference in the diagonal components of the specified Reynolds stress tensor used as anisotropy model for case 1. Also shown is the sound directivity as predicted by the statistical model (solid line). The level from the statistical model has been adjusted to match the peak level of the numerical results. One can see that the direction of the sound directivity is the same for the numerical results and the statistical model. The degree of directivity in terms of OASPL is however twice as large for the statistical model compared to the numerical results.

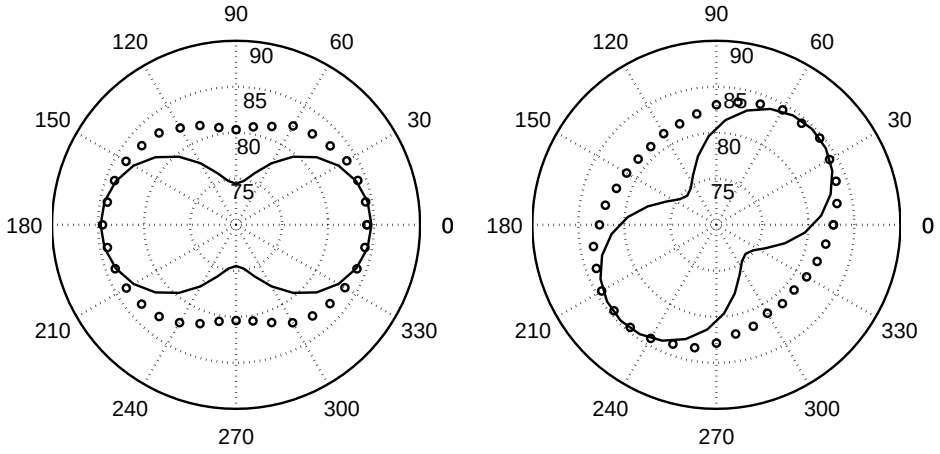

(a) Case 1 (b) Case 2

Figure 6. OASPL in xy-plane at radius $R = 100$ for angles $\theta = 0 : 10 : 360$ degrees. Circles: SNGR method; solid line: statistical model.

The OASPL at the same locations for case 2 are shown in Fig. 6(b). The direction of maximum sound emission is rotated by 45 degrees as specified by the Reynolds stress tensor used as anisotropy model for this case. The directivity is otherwise almost the same as in Fig. 6(a) indicating that the rotation operation only change the direction of the emitted sound and not the character of the sound field. The results in Figs. 6(a) and 6(b) indicate that the direction of maximum sound emission can be deduced from the Reynolds stress tensor when rotated into the principal axes. The sound emission is strongest in the direction of the largest normal component and weakest in the direction of the smallest one. These results hold for homogeneous turbulence which is not convected by a mean flow where a convective amplification would increase the noise generation in the downstream direction and reduce the emission in the upstream direction.

The reason for the difference in the sound emission directivity levels between the numerical results and the statistical model is unclear. It has been pointed out by Witkowska *et al.* [19] that unphysical end-effects may dominate the sound generation when source terms with spatial derivatives are used over a truncated source region. The directivity pattern from the stochastic anisotropic turbulence is probably partially masked by this effect which would explain the difference compared to the statistical model. The sound directivity would probably be in better agreement with the statistical model if this effect were removed in the computations. The statistical model for the velocity correlation tensor is however a simple modification of the isotropic expression and might be a too crude model to compare with. The true degree of sound directivity from anisotropic homogeneous turbulence can not be deduced from the present results.

The 1/3 octave power spectral density of the far-field pressure for case 1 is shown in Fig. 7. Spectra are shown for observer locations 1 and 10 (0 and 90 degrees). The effect of the anisotropy is clearly visible in the spectral content of the emitted sound. There is an increase of the sound at low frequencies for the direction of the largest normal component of the Reynolds stress tensor (0 degrees). The opposite is true for the direction of the smallest component (90 degrees). The frequency dependence is also changed to a more flat spectra at 90 degrees than at 0 degrees.

Since the reference solution in the linearized Euler equation solution is stagnant and only the Reynolds stress tensor model include anisotropy, only the self-noise is demonstrated. Therefore these results apply to the self-noise component of the emitted sound and not for the shear-noise component, see Ribner.[10]

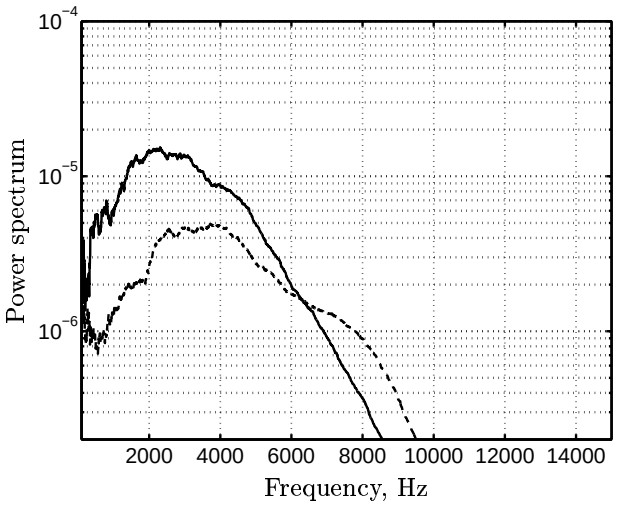

Figure 7. 1/3 **octave power spectral density of the far-field pressure. Case** 1. **Solid line: observer point** 1 (x^* **direction); dashed line: observer point** 10 (y^* **direction)**

Including shear in the solution to the linearized Euler equations is however numerically very difficult. This is due to natural instabilities of the linearized Euler equations and limitations of the validity of the Kirchhoff integration method in inhomogeneous flows.

IX. Conclusion

A method to generate anisotropic stochastic turbulence which is divergence free for the homogeneous case has been presented. The method includes anisotropy in velocities and length scales, but not in time scales of individual velocity components.

The length scale anisotropy of the proposed method is shown to be related to the relative magnitude of the diagonal Reynolds stress tensor components. As a result, the maximum and minimum length scales for homogeneous synthesized turbulence are found in the directions of the principal axes of the Reynolds stress tensor.

The directivity of the sound which is generated from the anisotropic synthesized has a clear directivity. The sound emission directivity is (as for the length scale) related to the relative magnitude of the diagonal Reynolds stresses with maximum and minimum directivity in the directions of the principal axes. The results from a statistical model for the sound generated from anisotropic homogeneous turbulence are in qualitative agreement with the numerical results. The sound pressure level directivity is though twice as large for the statistical model compared to the numerical results. Numerical errors related to a finite source region in the numerical simulations are believed to be the reason for the difference in directivity level. Further work is though needed for conclusive comparisons.

X. Acknowledgment

This work was conducted as part of NFFP (National Flight Research Program) as well as the EU 5th Framework Project JEAN (Jet Exhaust Aerodynamics & Noise), contract number G4RD-CT2000-000313.

References

[1]Billson, M., Eriksson, L.-E., and Davidson, L., "Jet Noise Prediction Using Stochastic Turbulence Modeling," The 9th AIAA/CEAS Aeroacoustics Conference, AIAA 2003-3282, Hilton Head, South Carolina, 2003.

[2]Bechara, W., Bailly, C., Lafon, P., and Candel, S. M., "Stochastic Approach to Noise Modeling for Free Turbulent Flows," *AIAA Journal*, Vol. 32 , No. 3, 1994, pp. 455–463.

[3]Bailly, C., Lafon, P., and Candel, S. M., "A Stochastic Approach to Compute Noise Generation and Radiation of Free Turbulent Flows," AIAA Paper 95-092, 1995.

[4]Bailly, C. and Juvé, D., "A Stochastic Approach To Compute Subsonic Noise Using Linearized Euler's Equations," AIAA Paper 99-1872, 1999.

[5]Smirnov, A., Shi, S., and Celik, I., "Random Flow Generation Technique for Large Eddy Simulations and Particle Dynamics Modeling," *ASME: Journal of Fluids Engineering*, Vol. 123, 2001, pp. 359 – 371.

[6]Batten, P., Goldberg, U., and Chakravarthy, S., "Interfacing Statistical Turbulence Closures with Large-Eddy Simulation," *AIAA Journal*, Vol. 42 (3), 2004, pp. 485–492.

[7]Lighthill, M., "On sound generated aerodynamically, I. General theory," *Proc. Roy. Soc.*, Vol. A 211, 1952, pp. 564–587.

[8]Billson, M., Eriksson, L.-E., and Davidson, L., "Acoustic Source Terms for the Linear Euler Equations on Conservative form," The 8th AIAA/CEAS Aeroacoustics Conference, AIAA 2002-2582, Breckenridge, Colorado, 2002.

[9]Pierce, A., *Acoustics. An Introduction to Its Physical Principles and Applications*, Acoustical Society of America, Woodbury, New York, 1991.

[10]Ribner, H., "Quadrupole correlations governing the pattern of jet noise," *Journal of Fluid Mechanics*, Vol. 38, 1969, pp. 1 – 24.

[11]Kraichnan, R., "Noise Transmission From Boundary Layer Pressure Fluctuations," *J. Acoust. Soc. Am.*, Vol. 29, 1957, pp. 65–80.

[12]Billson, M., Eriksson, L.-E., and Davidson, L., "Jet Noise Modeling Using Synthetic Anisotropic Turbulence," The 10th AIAA/CEAS Aeroacoustics Conference, AIAA 2004-3028, Manchester, United Kindom, 2004.

[13]Billson, M., "Computational Techniques for Jet Noise Predictions," *Lic. Thesis, Department of Thermo and Fluid Dynamics, Chalmers University of Technology, Gothenburg*, 2002.

[14]Lumley, J., "Computational Modeling of Turbulent Flows," *Adv. Appl. Mech.*, Vol. 18, 1978, pp. 123–176.

[15]Andersson, N., Eriksson, L.-E., and Davidson, L., "Large–Eddy Simulation of a Mach 0.75 Jet," The 9th AIAA/CEAS Aeroacoustics Conference, AIAA 2003-3312, Hilton Head, South Carolina, 2003.

[16]Batchelor, G., *The theory of homogeneous turbulence*, Cambridge University Press, 1953.

[17]Lilley, G., "On the noise from jets," *AGARD CP-131*, 1974.

[18]P. Jordan and Y. Gervais, "Modelling self and shear noise mechanisms in anisotropic turbulence," The 9th AIAA/CEAS Aeroacoustic Conference, AIAA 2003-8743, Hilton Head, South Carolina, 2003.

[19]A. Witkowska, D. J. and Brasseur, J. G., "Numerical Study of Noise From Isotropic Turbulence," *Journal of Computational Acoustics*, Vol. 5 (3), 1997, pp. 317–336.